Influence Analysis of Secondary O-ring Seals in Dynamic Behavior of Spiral Groove Gas Face Seals

HU Songtao, HUANG Weifeng, LIU Xiangfeng*, and WANG Yuming

State Key Laboratory of Tribology, Tsinghua University, Beijing 100084, China

Abstract: The current research on secondary O-ring seals used in mechanical seals has begun to focus on their dynamic properties. However, detailed analysis of the dynamic properties of O-ring seals in spiral groove gas face seals is lacking. In particular a transient study and a difference analysis of steady-state and transient performance are imperative. In this paper, a case study is performed to gauge the effect of secondary O-ring seals on the dynamic behavior (steady-state performance and transient performance) of face seals. A numerical finite element method (FEM) model is developed for the dynamic analysis of spiral groove gas face seals with a flexibly mounted stator in the axial and angular modes. The rotor tilt angle, static stator tilt angle and O-ring damping are selected to investigate the effect of O-ring seals on face seals during stable running operation. The results show that the angular factor can be ignored to save time in the simulation under small damping or undamped conditions. However, large O-ring damping has an enormous effect on the angular phase difference of mated rings, affecting the steady-state performance of face seals and largely increasing the possibility of face contact that reduces the service life of face seals. A pressure drop fluctuation is carried out to analyze the effect of O-ring seals on the transient performance of face seals. The results show that face seals could remain stable without support stiffness and O-ring damping during normal stable operation but may enter a large-leakage state when confronting instantaneous fluctuations. The oscillation-amplitude shortening effect of O-ring damping on the axial mode is much greater than that on the angular modes and O-ring damping prefers to cater for axial motion at the cost of angular motion. This research proposes a detailed dynamic-property study of O-ring seals in spiral groove gas face seals, to assist in the design of face seals.

Keywords: spiral groove, gas face seal, secondary O-ring seals, dynamic property

1 Introduction

Spiral groove gas face seals (in Fig. 1) are a type of non-contacting mechanical face seal to obstruct sealed gas from escaping from one compartment to another. Elastomeric O-rings are widely used as secondary O-ring seals in face seals for they are economical and effective over a broad range of service conditions and surface finishes. As the damping of secondary O-ring seals is a significant parameter to make up a rotor system together with the stiffness of support spring and the characteristics of gas film, the properties of O-rings (static property and dynamic property) have a remarkable influence on the properties of face seals. MOONEY[1] provided a theory about the large elastic deformation of isotropic materials. His theory was complemented by RIVLIN[2] and tested by TRELOAR[3]. LINDLEY[4–5] first assumed plane strain conditions and obtained a nondimensional force deflection relationship for an O-ring. GREEN, et al[6], then researched

the axial and radial compression of O-rings, and proposed axisymmetric analyses which are different from plane strain conditions.
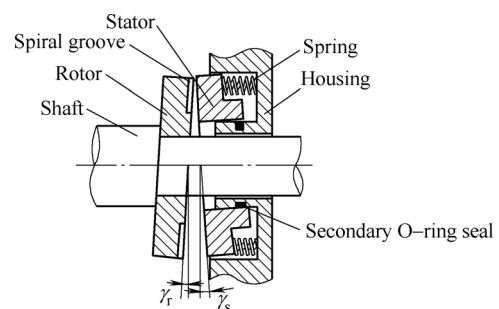

Fig. 1.   Schematic of a typical spiral groove face seal

Based on an understanding of the static properties of O-rings, researchers started to pay more attention to the dynamic properties of secondary O-ring seals in practical mechanical seals. GREEN, et al[7], experimentally measured stiffness and damping coefficients using a frequency excitation method and investigated the effects of squeeze and pressure on the dynamic characteristics of O-rings. LEE, et al[8], introduced a new method of modeling and measuring the stiffness and damping of elastomeric O-ring secondary

seals in a flexibly mounted stator seal. GREEN, et al[9–10], showed that high stiffness and damping increased the critical speed, and presented a parametric analysis to gauge the influence of stiffness and damping on the steady-state performance of coned-face gas seals. However, with regard to the dynamic properties of O-ring seals, current works lack of detailed analyses for spiral groove gas face seals, especially for their transient performance. Moreover, none of these studies have provided a difference analysis of O-ring seals between steady-state performance and transient performance of face seals.

Proper sealing dynamics is needed before the dynamic properties of O-rings can be properly analyzed. The dynamics of mechanical seals has been active as the works by ETSION[11–13]. SHAPIRO, et al[14], and LEEFE[15] solved lubrication and dynamics equations individually when studying the dynamics. ZIRLELBACK, et al[16], acquired the linearized stiffness and damping coefficients of spiral groove gas face seals by using a perturbation method, and then ZIRLELBACK[17] utilized this method to present a corresponding parametric analysis. MILLER, et al[18], developed a method to solve lubrication and dynamics equations simultaneously by transforming them into a state space form considering both axial and angular modes of motion. This method was adopted by GREEN, et al[9–10] to study non-contacting coned-face mechanical seals during stable running operation, and RUAN[19–20] to study spiral groove gas face seals during startup and shutdown operations.

In this work, a numerical model is developed for the dynamic analysis of spiral groove gas face seals with a flexibly mounted stator in the axial and angular modes. A detailed analysis of O-ring damping is carried out to gauge its influence on the steady-state performance of face seals during stable running operation. A further analysis about the influence of O-rings on the transient performance of face seals during a pressure drop fluctuation is performed and a difference analysis of O-ring seals between the steady-state performance and transient performance of face seals is presented.

2   Sealing Dynamics

The dynamics of a spiral groove face seal is shown in Fig. 2[18]. As the rotor and stator tilt angles are small, the angles can be treated as vectors. Here the rotor tilt angle γ_r, stator tilt angle γ_s and relative tilt angle γ_{rel} can be decomposed into components along the X and Y axes:

$$\begin{cases} \boldsymbol{\gamma}_r = (\gamma_r \cos(\omega t),\, \gamma_r \sin(\omega t)), \\ \boldsymbol{\gamma}_s = (\gamma_x,\, \gamma_y), \\ \boldsymbol{\gamma}_{rel} = \boldsymbol{\gamma}_r - \boldsymbol{\gamma}_s. \end{cases} \tag{1}$$

The geometry of the rotor is depicted in Fig. 3. A total of N spiral grooves are processed on the rotor at a depth of δ_g.

The groove width to the land width fraction is λ, and the groove length to the dam length fraction is β. α is the spiral angle varying from 0 to 180°. r_o, r_i and r_g are respectively outer radius, inner radius and the boundary for groove region and dam region.
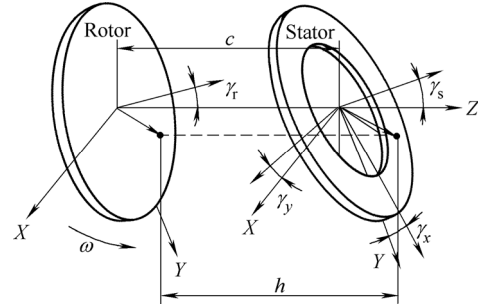

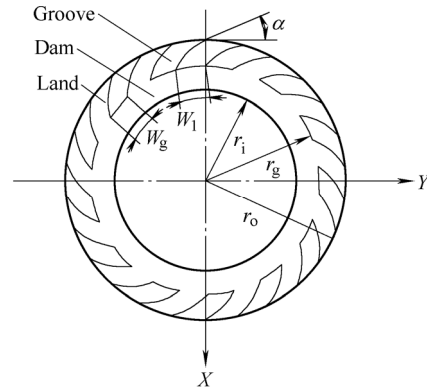Fig. 2.   Kinematic model of the spiral groove face seal

Fig. 3.   Spiral groove geometry profile

The gas film thickness of any point (x, y) on the stator face is given by

$$h(x, y) = c + y\gamma_x - x\gamma_y - \gamma_r y \cos(\omega t) + \gamma_r x \sin(\omega t) + \langle \delta_g \rangle, \tag{2}$$

where c is the gas film thickness at the central point, and $\langle \delta_g \rangle$ indicates a δ_g-deep groove in the groove region.

Considering the stiffness and damping property of springs and the secondary seal, the dynamics equations for axial and angular modes are given by[20–21]

$$\begin{cases} m\ddot{c} + c_{sz}\dot{c} + k_{sz}c = -F_{closing} + F_g, \\ I\ddot{\gamma}_x + c_{s\gamma}\dot{\gamma}_x + k_{s\gamma}\gamma_x = M_{gx} + M_{si}, \\ I\ddot{\gamma}_y + c_{s\gamma}\dot{\gamma}_y + k_{s\gamma}\gamma_y = M_{gy}, \end{cases} \tag{3}$$

where m and I are the mass and the transverse moment of inertia of the stator. M_{si} is a moment caused by the static stator tilt, which is arbitrarily assumed to be about the X axis. The constant moment is given by $M_{si}=k_{s\gamma}\gamma_{si}$. k_{sz} is the axial stiffness of springs and c_{sz} is the damping property of flexible support. According to GREEN, et al[21], the angular stiffness $k_{s\gamma}$ and damping $c_{s\gamma}$ are given by

$$k_{s\gamma} = \frac{1}{2} k_{sz} \cdot r_{\mathrm{o}}^2, \ c_{s\gamma} = \frac{1}{2} c_{sz} \cdot r_{\mathrm{o}}^2. \tag{4}$$

Assuming that the support forces act at the outer radius. The force F_{closing} is the total load of the fluid pressure and the spring support load at the equilibrium state that is applied to the rear side of the stator to balance the gas film load F_g caused by the hydrostatic and hydrodynamic effects. All load and moments can be obtained by integrating the gas film pressure p over the sealing area A defined as

$$F_g = \int_A p \mathrm{d}A, \ M_{gx} = \int_A py\mathrm{d}A, \ M_{gy} = -\int_A px\mathrm{d}A. \tag{5}$$

The gas pressure distribution is governed by lubrication equation. Assuming gas flow is ideal, isothermal, and unrelated to surface roughness, the compressible Reynolds equation is given by[22]

$$\vec{\nabla} \cdot \left[ph^3 \vec{\nabla} p - 6\mu\omega rph \boldsymbol{i}_\theta \right] - 12\mu \frac{\partial(ph)}{\partial t} = 0, \tag{6}$$

where μ is the gas viscosity and ω is the shaft speed. The boundary conditions to Eq. (6) are

$$p(r = r_{\mathrm{i}}) = p_{\mathrm{i}}, \ p(r = r_{\mathrm{o}}) = p_{\mathrm{o}}. \tag{7}$$

The corresponding rectangular form of Eq. (7) is

$$\vec{\nabla} \cdot \left[ph^3 \vec{\nabla} p + 6\mu\omega ph(y\boldsymbol{i}_x - x\boldsymbol{i}_y) \right] - 12\mu \frac{\partial(ph)}{\partial t} = 0. \tag{8}$$

To sum up, a complete chain is established for the coupling process of lubrication and dynamics. $h(x, y)$ can be gathered from Eq. (2) based on the current axial position and angular orientation. Then the current gas film pressure profile p could be calculated using the lubrication equation Eq. (8) with the boundary conditions given by Eq. (7). After integrating the current gas film pressure p over the sealing area A according to Eq. (5), the current face load can be substituted into dynamics equation Eq. (3) to obtain the next time step value for $h(x, y)$.

The numerical model of gas face seals is calculated by using FEM. Numerical accuracy and stability are important for the dynamic analysis of a complex system. A very fine meshing and a very small time step would make the computation time consuming. Therefore a balance between the accuracy and economic computing should be maintained. After experiments, it is finally determined that a time step of 1×10^{-6} s (ω=5000 r/min) with a 3160 finite element mesh is adopted. The computation is performed on a 2.3 GHz PC.

3 Results and Discussion

In the study of steady-state performance, a detailed parametric analysis of O-ring damping is performed to gauge its influence on the steady-state performance of face seals during stable running operation. A pressure drop fluctuation (p_{o} decompresses from 1 MPa to 0.1 MPa at 0.012 s) is then introduced to research the influence on the transient performance of face seals. A corresponding difference analysis of O-ring seals between steady-state performance and transient performance of face seals is presented. Here the pressure drop fluctuation could appear when there is a gas supply failure or a gas pipe break.

Four evaluation indexes are chosen: the gas film thickness at center c to assess the axial position of the stator, the relative tilt angle γ_{rel} to assess the tracking property of the stator in the angular modes in the transient response, the transmissibility $|\gamma_{\mathrm{rel}}/\gamma_{\mathrm{r}}|$ to replace γ_{rel} in the steady-state response[23], and the leakage Q to assess the sealing property. c and $\gamma_{\mathrm{rel}}(|\gamma_{\mathrm{rel}}/\gamma_{\mathrm{r}}|)$ are a type of indexes to reflect the potential possibility of face contact. Both could be used to assess the property of service life which is distinguished from the sealing property assessment index Q.

To start the calculation of dynamic models, the initial axial position, angular orientation and force profile are needed to be computed first. The initial conditions for the stator are chosen so that the stator and the rotor are in perfect alignment. This condition requires that $\gamma_x = \gamma_r$, $\gamma_y = \dot{\gamma}_x = \dot{c} = 0$, $\dot{\gamma}_y = \omega\gamma_r$ and $c = c_0$. To compute the initial axial position c_0 and initial pressure profile, a simple numerical model is established so that the closing load on the rear of the stator caused by pressure drop and springs is equal to the opening load on the sealing face of the stator provided by the fluid effect. This model considers only axial mode and is based on the assumption that the rotor and the stator are in perfect alignment above. Table 1 illustrates a fundamental parameter case. In the Fundamental Case, some geometry parameters are non-integral because they correspond to a test rig while the varied parameters subsequently are carried one level deeper.

Table 1. Parameters of fundamental case

Parameter	Value
Outer radius r_{o}/m	0.061 7
Inner radius r_{i}/m	0.051 6
Balance radius r_{b}/m	0.053 05
Spiral angle α/(°)	15
Number of grooves N	12
Groove to land width ratio λ	0.5
Groove to dam length ratio β	0.6
Groove depth δ_{g}/μm	6
Stator mass m/kg	0.13
Transverse moment of inertia I/(kg • m^2)	2.5×10^{-4}
Pressure at outer radius p_{o}/MPa	1
Pressure at inner radius p_{i}/MPa	0.1
Shaft speed ω/(r • min^{-1})	5000
Support axial stiffness k_{sz}/(kN • m^{-1})	16.4
Support angular stiffness $k_{s\gamma}$/(N • m • rad^{-1})	31
Support axial damping c_{sz}/(N • s • m^{-1})	0
Support angular damping $c_{s\gamma}$/(N • m • s • rad^{-1})	0
Rotor tilt angle γ_{r}/μrad	0
Static stator tilt angle γ_{si}/μrad	0

3.1 Steady-state performance

The rotor is rigidly mounted on the shaft and its tilt angle is result of manufacturing or assembly imperfections. The stator itself also has a static tilt angle due to imperfections in its flexible support. As both of them are significant to the steady-state performance of face seals, they are chosen as the reference for comparison with the O-ring damping to measure the level of influence of damping. In Table 2, 16 cases are referenced by ij, where i refers to the cluster number, and j refers to the variation within the cluster. The cases are computed according to $i=1–4$, and the last of the former cluster is the first of the latter cluster. For instance, if $i=1$ and $j=1$ then Case 11 corresponds to the Fundamental Case. Subsequently j increases until it arrives at 4, which corresponds to the increase of the rotor tilt angle γ_r from 0 to 1000 µrad. Then i transforms from 1 to 2 and j returns to 1. Here Case 21 is equal to Case 14, and starts to change the value of the static stator tilt angle γ_{si} in the cluster of $i=2$.

Table 2.   Cases for steady-state performance investigation

| Case number	Parameter to vary		
	Rotor tilt angle γ_r/µrad	Static stator tilt angle γ_{si}/µrad	Support axial damping c_{sz}/(N·s·m^{-1})
	$i=1$	$i=2$	$i=3$
$j=1$	0	0	0
$j=2$	50	50	50
$j=3$	500	500	500
$j=4$	1000	1000	1000
$j=5$	–	–	2000
$j=6$	–	–	3000
$j=7$	–	–	4000
$j=8$	–	–	5000

3.1.1 Investigation of tilt angle

The rotor tilt angle is investigated first in Cases 11–14. In Fig. 4, Case 11 acts as the Fundamental Case because its rotor tilt angle and static stator tilt angle are zero. It is evident from Fig. 4 that film thickness at center, relative tilt angle and leakage depart from the results of Case 11 and the distance expands with the increase of rotor tilt angle. However, even when the rotor tilt angle reaches 1000 µrad which is unacceptable in practical applications, the value of the distance is still quite small. After the rotor tilt angle reaches 1000 µrad, the static stator tilt angle starts to vary from 0 to 1000 µrad in Cases 21–24. It is obvious that film thickness at center, relative tilt angle and leakage depart from the results of Case 14 or 21 (γ_r=1000 µrad, γ_{si}=0 µrad) and the distance expands with the increase of static stator tilt angle. The value of the distance is also quite small, similar to the rotor tilt angle. Fig. 4(d) shows a typical synchronous effect mechanism of two tilt angles at a steady state from 0.006 s to 0.024 s. As depicted in the figure, the average value is the stator steady-state response only to the rotor tilt angle and the oscillation is the stator steady-state response to its own tilt angle. Here the transmissibility in Fig. 4(b) is modified by $|\gamma_{rel}/\gamma_r|_{max}=(|\gamma_{rel,r}|+|\gamma_{rel,si}|)/|\gamma_r|$ when
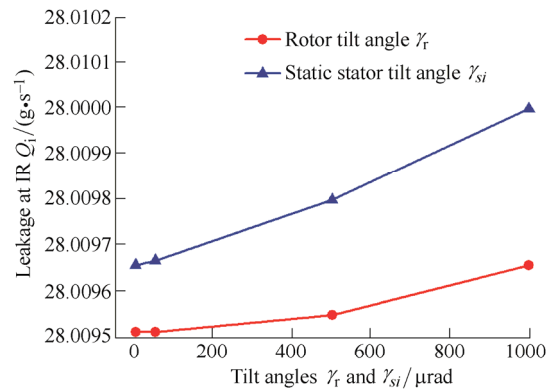
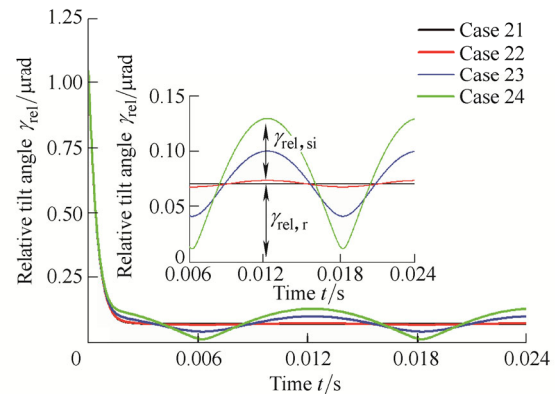the influence of static stator tilt angle is involved.
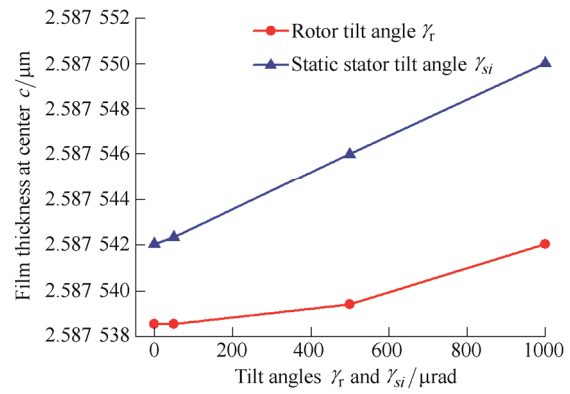
(a) Film thickness at center c of Cases 11–24
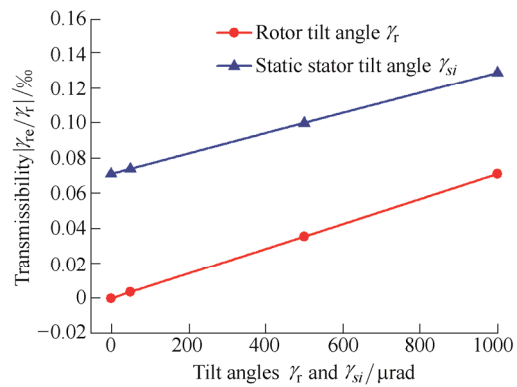
(b) Transmissibility $|\gamma_{rel}/\gamma_r|$ of Cases 11–24

(c) Leakage at IR Q_i of Cases 11–24

(d) Synchronous effect mechanism of tilt angles at a steady state

Fig. 4.   Influence of tilt angles on the steady-state performance of face seals

It is concluded from Fig. 4 that the influence of rotor tilt angle and static stator tilt angle on the steady-state performance of face seals is insignificant under undamped or small damping conditions. When ignoring tilt angles in the angular modes, the steady-state simulation result would deviate from the real condition but the error is small so that it can be ignored. Therefore, an axial seal model could be adopted in the research of face-seal steady-state performance for time saving under undamped or small damping conditions.

3.1.2 Investigation of damping

It is quite clear in Figs. 5(a) and 5(b) that an oscillation appears on film thickness at center in Cases 31–38 similar to relative tilt angle in Fig. 4(d). The corresponding relative tilt angle curves in Figs. 5(c) and 5(d) do not arrive at the extreme points at the same time as the curves do in Fig. 4(d). Moreover, it is found that O-ring damping will affect the steady-state performance of face seals in the angular modes. Fig. 5(e) provides a close look at γ_x and γ_{rx} for Case 38 under steady-state condition, which respectively represents the stator tilt angle and the rotor tilt angle component along the X axis. It can be seen that the large O-ring damping will induce a large phase difference between the stator and the rotor in the angular modes to impact the steady-state performance of face seals. It is obvious in Fig. 5(g) that transmissibility arrives at nearly 1‰ when damping is 500 N • s/m, which is much more remarkable than those of two tilt angles.

(a) Film thickness at center c of Cases 31–38

(b) Magnification of (a)

(c) Relative tilt angle γ_{rel} of Cases 31–38

(d) Magnification of (c)

(e) Tile angles γ_{rx} and γ_x

(f) Film thickness at center c of Cases 31–38

(g) Transmissibility $|\gamma_{rel}/\gamma_r|$ of Cases 31–38

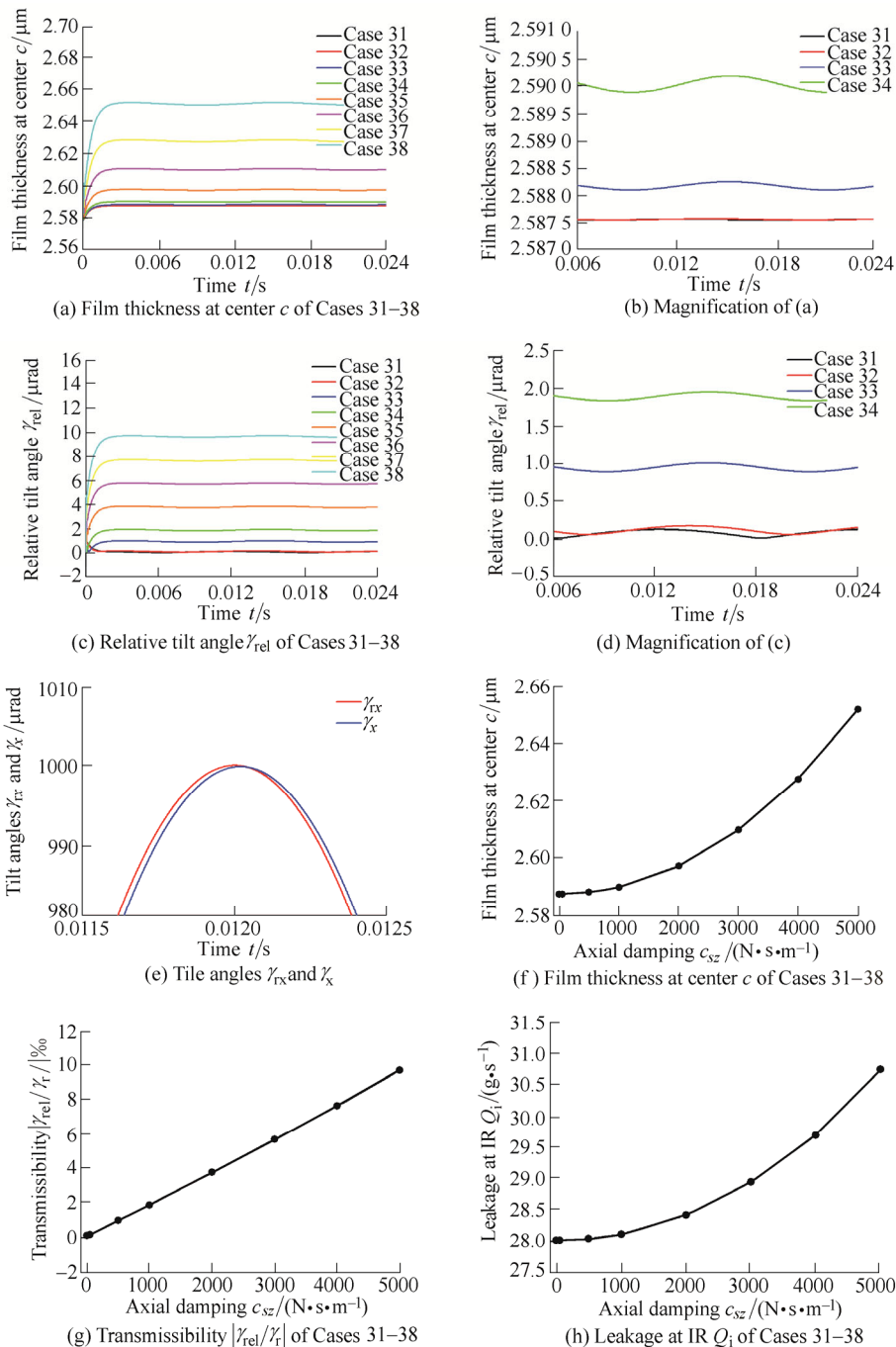(h) Leakage at IR Q_i of Cases 31–38

Fig. 5. Influence of the damping of O-ring seal on the steady-state performance of face seals

As described in the analysis of the two tilt angles above, an axial seal model could be adopted to take place of an axial-angular seal model for time saving. However, this conclusion is established based on the assumption that O-ring damping is small or zero. It is apparent that when the two tilt angles are ignored under large damping conditions, the enormous effect of damping on the phase difference in the angular modes will be lost, which is effective for the steady-state performance of face seals. Therefore, it is concluded that rotor tilt angle and static stator tilt angle cannot be ignored under large damping conditions even if the influence of tilt angles is feeble. In addition, this phenomenon of the phase difference will largely increase the possibility of face contact which may reduce the service life of seals. It is another reason why the angular factor should not be ignored for time saving.

3.2　Transient performance

Cases 41–46 in Table 3 select parameters of the Fundamental Casein Table 1, while $\gamma_r=1000$ μrad and the value of stiffness and damping varies. A pressure drop fluctuation (p_o decompresses from 1 MPa to 0.1 MPa at 0.012 s) is carried out to investigate the influence of O-ring damping on the transient performance of face seals. As Cases 42–44 are extreme conditions and their transient responses have different orders of magnitude from other normal conditions, they are discussed individually.

Table 3.　Cases for transient performance investigation

Case number	Parameter to vary $i=4$
	Support axial stiffness k_{sz}/(N · m^{-1}),
	Support axial damping c_{sz}/(N · s · m^{-1})
$j=1$	16.4×10^3, 300
$j=2$	0, 0
$j=3$	16.4×10^3, 0
$j=4$	0, 300
$j=5$	16.4×10^4, 300
$j=6$	16.4×10^3, 3000

In Figs. 6(a) and 6(b), it is obvious that before the appearance of pressure drop fluctuation (0.012 s), film thickness at center and relative tilt angle are nearly zero, that means the stator can track the rotor well and the face seal works stably at steady state even if there is no support stiffness and O-ring damping. When the fluctuation arrives at 0.012 s, film thickness at center increases rapidly to about 200 μm and relative tilt angle also increases to about 2500 μrad. This implies the instantaneous decrease of pressure load on the rear of the stator induces the stator to be pushed far away from the rotor and oscillate violently in the angular modes. As there is no support stiffness nor O-ring damping in Case 42 to weaken the motions above, the order of magnitude of film thickness at center and relative tilt angle are much greater than those at a stable running state within the computing time (0.06 s). In Figs. 6(c), 6(d), Case 43 with only support stiffness oscillates severely on film thickness and relative tilt angle while it is able to recover to a stable state again. Conversely, Case 44 with only O-ring damping placidly comes to a large film thickness at center for the absorbing effect of damping. The oscillation vanishes in the axial mode but enhances in the angular modes.

Figs. 6(e)–6(g) are about the comparative analysis of normal cases. It is evident that support stiffness aggravates the oscillation times and shortens the oscillation amplitude in the axial and angular modes. However, O-ring damping weakens the oscillation times and shortens the oscillation amplitude. Here, the oscillation-amplitude shortening effect in the angular mode is much feebler. Considering the results of Case 44, it seems that O-ring damping prefers to cater for axial motion at the cost of angular motion. With regard to leakage, stiffness and O-ring damping are both helpful to minimize leakage oscillation during the fluctuation while the effect of large damping is much more considerable.

Hence, it is concluded first that face seals could remain stable without support stiffness and O-ring damping during normal operation, but may enter a large-leakage state or even seal failure when confronting excessive fluctuations instantaneously. Second, the oscillation-amplitude shortening effect of O-ring damping in the axial mode is much more considerable than that in the angular modes, which is different from the same obvious oscillation-amplitude shortening effect of support stiffness both in the axial and angular modes. O-ring damping seems to prefer to cater for axial motion at the cost of angular motion.

4　Conclusions

(1) A numerical model is developed for the dynamic analysis of spiral groove gas face seals with a flexibly mounted stator in the axial and angular modes.

(2) The steady-state performance research shows the following. a) When O-ring damping is small or zero, the angular factor can be ignored for time saving in the simulation. b) Large O-ring damping has an enormous effect on the phase difference in the angular modes to affect the steady-state performance of face seals even if the influence of tilt angles is feeble. Phase difference is a phenomenon that largely increases the possibility of face contact to reduce the service life of seals. Therefore, the angular factor should not be ignored under large damping conditions.

(3) The transient performance research shows the following. a) Face seals can remain stable without support stiffness and O-ring damping during normal stable operation but may enter a large-leakage state when confronting excessive fluctuations instantaneously. b) The oscillation-amplitude shortening effect of O-ring damping in the axial mode is much more considerable than that in the angular modes, which is different from the same obvious oscillation-amplitude shortening effect of support stiffness both in the axial and angular modes. O-ring

damping seems to prefer to carter for axial motion at the cost of angular motion.
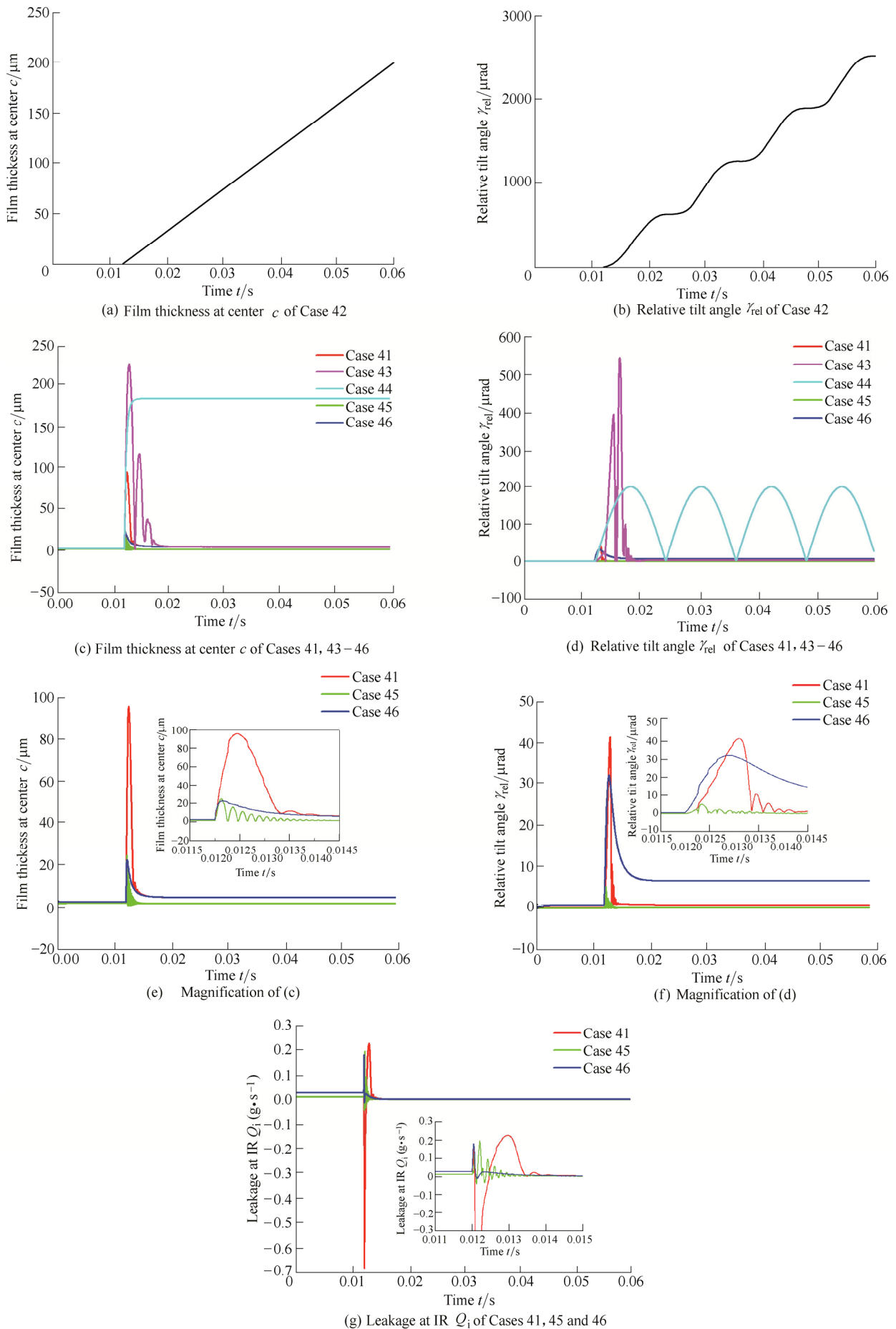

(a) Film thickness at center c of Case 42

(b) Relative tilt angle γ_{rel} of Case 42

(c) Film thickness at center c of Cases 41, 43−46

(d) Relative tilt angle γ_{rel} of Cases 41, 43−46

(e) Magnification of (c)

(f) Magnification of (d)

(g) Leakage at IR Q_i of Cases 41, 45 and 46

Fig. 6. Influence of the damping of O-ring seal on the transient performance of face seals

References

[1] MOONEYM. A theory of large elastic deformation[J]. *Journal of Applied Physics*, 1940, 11(9): 582–592.

[2] RIVLIN R S. Large elastic deformations of isotropic materials. Ⅰ.fundamental concepts[J]. *Philosophical Transactions of the Royal Society*, 1948, 240(822): 379–397, 459–490, 509–525.

[3] TRELOAR L R G. Stress-strain data for vulcanized rubber under various types of deformations[J]. *Rubber Chemistry & Technology*, 1944, 17(4): 813–825.

[4] LINDLEY P B. Load-compression relationships of rubber units[J]. *The Journal of Strain Analysis for Engineering Design*, 1966, 1(3): 190–195.

[5] LINDLEY P B. Compression characteristics of laterally unrestrained rubber O-ring[J]. *Journal International Rubber Institute*, 1967, 1: 202–213.

[6] GREEN I, ENGLISH C. Analysis of elastomeric O-ring seals in compression using the finite element method[J]. *Tribology Transactions*, 1992, 35(1): 83–88.

[7] GREEN I, ETSION I. Pressure and squeeze effects on the dynamic characteristics of elastomer O-rings under small reciprocating motion[J]. *Journal of Tribology*, 1986, 108(3): 439–445.

[8] LEE A S, GREEN I. Physical modeling and data analysis of the dynamic response of a flexibly mounted rotor mechanical seal[J]. *Journal of Tribology*, 1995, 117(1): 130–135.

[9] GREEN I, BARNSBY R M. A simultaneous numerical solution for the lubrication and dynamic stability of noncontacting gas face seals[J]. *Journal of Tribology*, 2001, 123(2): 388–394.

[10] GREEN I, BARNSBY R M. A parametric analysis of the transient forced response of noncontacting coned-face gas seals[J]. *Journal of Tribology*, 2002, 124(1): 151–157.

[11] ETSION I. A review of mechanical face seal dynamic[J]. *Shock and Vibration*, 1982, 14(3): 9–14.

[12] ETSION I. Mechanical face seal dynamics update[J]. *Shock and Vibration*, 1985, 17(4): 11–16.

[13] ETSION I. Mechanical face seal dynamics 1985–1989[J]. *Shock and Vibration*, 1991, 23(4): 3–7.

[14] SHAPIRO W, COLSHER R. Steady-state and dynamic analysis of a jet engine, gas lubricated shaft seal[J]. *ASLE Transactions*, 1974, 17(3): 190–200.

[15] LEEFE S. Modeling of plain face gas seal dynamics[C]//*14th International Conference on Fluid Sealing, BHR Group Conference Series*, Suffolk, UK, 1994, (9): 397–424.

[16] ZIRKELBACK N, ANDRESL S. Effect of frequency excitation on force coefficients of spiral groove gas seals[J]. *Journal of Tribology*, 1999, 121(4): 853–863.

[17] ZIRKELBACK N. Parametric study of spiral groove gas face seals[J]. *Tribology Transactions*, 2000, 43(2): 337–343.

[18] MILLER B A, GREEN I. Numerical formulation for the dynamic analysis of spiral-grooved gas face seal[J]. *Journal of Tribology*, 2001, 123(2): 395–403.

[19] RUAN B. Numerical analysis of spiral groove gas seals under transient conditions[C/CD]//*56th STLE Annual Meeting*, Orlando, Florida, USA, May 20–24, 2001.

[20] RUAN B. Numerical modeling of dynamic sealing behaviors of spiral groove gas face seals[J]. *Journal of Tribology*, 2002, 124(1): 186–195.

[21] GREEN I, ETSION I. Stability threshold and steady-state response of noncontacting coned-face seals[J]. *ASLE Transactions*, 1985, 28(4): 449–460.

[22] GROSS W A. *Fluid film lubrication*[M]. New York: John Wiley & Sons, 1980.

[23] MILLER B A, GREEN I. Semi-analytical dynamic analysis of spiral-grooved mechanical gas face seals[J]. *Journal of Tribology*, 2003, 125(3): 403–413.

Biographical notes

HU Songtao, born in 1989, is a PhD candidate at *Department of Mechanical Engineering, Tsinghua University, China*. His research interest is mechanical seals.
Tel: +86-18811364107; E-mail: HSTTAOTAO@163.com

HUANG Weifeng, born in 1978, is currently an associate professor at *Department of Mechanical Engineering, Tsinghua University, China*. His research interest is mechanical face seals.
Tel: +86-10-62795124; E-mail: huangwf@tsinghua.edu.cn

LIU Xiangfeng, born in 1961, is currently a professor and a PhD candidate supervisor at *Department of Mechanical Engineering, Tsinghua University, China*. His research interest is machine design and mechanical face seals.
Tel: +86-10-62795122; E-mail: liuxf@tsinghua.edu.cn

WANG Yuming, born in 1941, is currently a professor and a PhD candidate supervisor at *Department of Mechanical Engineering, Tsinghua University, China*, and an academician of *Chinese Academy of Engineering*. His research interest is the fluid sealing technology.
Tel: +86-10-62771865; E-mail: yumingwang@tsinghua.edu.cn